A DUAL-BAND IMPEDANCE TRANSFORMER US-ING PI-SECTION STRUCTURE FOR FREQUENCY-DEPENDENT COMPLEX LOADS

X. F. Zheng[*], Y. A. Liu, S. L. Li, C. P. Yu, Z. R. Wang, and J. C. Li

School of Electronic Engineering, Beijing University of Posts and Telecommunications, Beijing, China

Abstract—In this paper, a new approach to build a dual-band impedance transformer is presented. The transformer can handle impedances that are complex and vary with frequency. This transformer contains a Pi-section structure, which can be equivalent to having two different electrical lengths at the two operating frequencies. One of the electrical lengths serves as complementary angle of the other. In this way, the conjugate impedances obtained through previous process are transformed to real impedance concurrently. All parameters are derived from closed-form equations. In addition, several simulations as well as a fabricated power amplifier (PA) are presented to verify the proposed transformer. The measured result performs a good agreement with the simulated one in return loss and gain. This transformer may find use in different stages of a transceiver such as power amplifiers which operate at two independent frequencies.

1. INTRODUCTION

Wireless communication plays an important role in human life. With the number of users increasing, new frequency bands are distributed for wireless communication, such as the emergence of new bands in Global System for Mobile communications (GSM) named GSM1800 and GSM1900, as well as 3rd generation communication. In addition, many wireless services present a characteristic of multi-band operation, the Wireless Local Area Networks (WLAN), for example, operates at both 2.4 GHz and 5.8 GHz. Furthermore, the coming long term evolution (LTE), which will operate at multi-band, serves as a demonstration

of the increasing prevalence of multi-band application. In fact, people have developed a lot of dual-band microwave components [1–7]. To cater the dual-band application, the impedance matching networks, which are essential in different stages of a RF transceiver, should then be transformed to multi-band impedance matching networks. To be more precise, the multi-band impedance matching should be achieved using only one set of matching networks.

In recent years, much attention was paid on the configuration of dual-band matching networks. In 2002, Y. L. Chow and K. L. Wan developed a two-section 1/3-wavelength transformer that operated at the fundamental frequency and its first harmonic [8]. Then Monzon enhanced the structure so that the two frequencies can be independent [9]. Also, Chebyshev impedance transformer provided a way to transform real impedance at dual-band [10, 11]. Besides, a Pi-structure transformer was developed to match real impedance at two arbitrary frequencies [12]. However, these can just find use in real impedance case. In most cases, such as power amplifier, the source impedances and the load impedances are usually complex and vary with frequency. To meet the requirement, some methods to match complex impedance are used [13–21]. In [13], impedances at each frequency were transformed to be identical real impedance using a transmission line and two stubs and then the two-section transformer in [9] was employed. Composite right/left-handed (CRLH) transmission lines were also used to match two frequency-dependent impedances [14]. In [15], a three-section impedance transformer was used to deal with the problem. Also, the structure of T-section impedance transformer was proposed [16], in which, two serial transmission lines with a stub in the junction transformed frequency-dependent complex loads to real impedance. In addition, Rawat and Ghannouchi employed the structure which acted as 90° transformers at both frequencies while bearing different characteristic impedances [17]. In [18], a dual-band impedance transformer using two-section shunt stubs was proposed, in which the high impedances were avoided by assigning the characteristic impedances of transmission lines first. The methodology of matching complex load impedance to complex source impedance was also proposed in [19]. The authors used lumped circuits to match frequency-dependent complex impedances according to the locations of the impedances when symbolizing them in Smith chart [20]. Even a hex-band power amplifier was developed using specific numerical method to determine the parameters of the matching networks [21].

In this paper, a transformer containing a Pi-section structure is proposed to match frequency-dependent complex loads to real
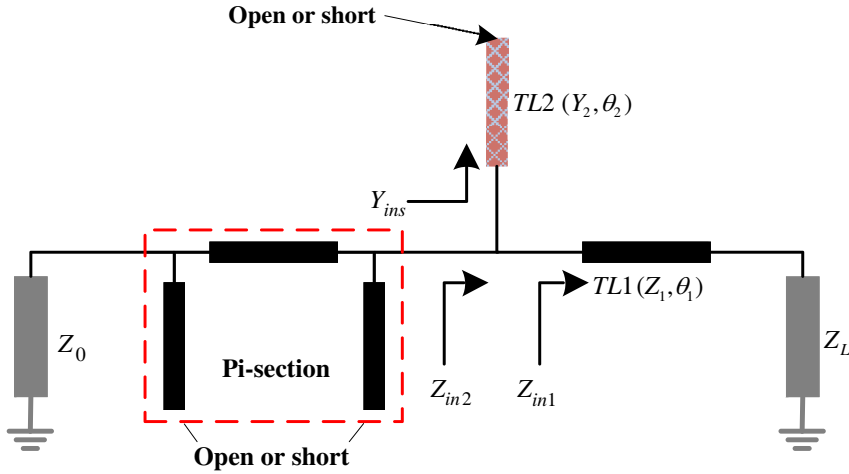
Figure 1. Topology of proposed dual-band impedance transformer.

impedance at both the operating frequencies concurrently. Closed form equations are used to determine the parameters of each section. To verify the design, a 900/2140 MHz dual-band power amplifier is realized with input/output matching networks designed based on the proposed methodology. A good agreement between simulation and measurement is obtained.

2. DUAL-BAND IMPEDANCE TRANSFORMER

Figure 1 shows the topology of the proposed dual-band impedance transformer. The proposed transformer is designed to match frequency-dependent impedances to real impedance Z_0 (mostly $50\,\Omega$ or $75\,\Omega$ in practice) at both frequencies.

In Figure 1, Z_L represents the load impedance. Usually it is complex and varies with frequency. So we can just rewrite it as follow:

$$Z_L = \begin{cases} Z_{L1} = R_{L1} + j \times X_{L1} & \text{at } f_1 \\ Z_{L2} = R_{L2} + j \times X_{L2} & \text{at } f_2 \end{cases} \tag{1}$$

Here in this paper, f_1 and f_2 represent the two operating frequencies. Generally, there is no relationship between f_1 and f_2 (f_2 is assumed to be larger than f_1). Besides, Z_L is frequency-dependent. Therefore, R_{L1} and R_{L2} as well as X_{L1} and X_{L2} are not related, respectively. TL1, TL2 and the Pi-section structure form the proposed dual-band impedance transformer. Several procedures are done before the whole matching process is achieved. Specifically, TL2 is not always needed, so a different symbol is used to denote TL2.

2.1. TL1

TL1 acts as a pre-transformer, which transforms the two independent impedances to conjugate ones. The process can be done by properly choosing TL1. The characteristic impedance and electrical length of TL1 can be determined using the following formulas [15]:

$$Z_1 = \sqrt{R_{L1} \times R_{L2} + X_{L1} \times X_{L2} + \frac{X_{L1} + X_{L2}}{R_{L2} - R_{L1}} \times (R_{L1} \times X_{L2} - R_{L2} \times X_{L1})} \quad (2)$$

$$\theta_1 = \arctan\left[\frac{Z_1 \times (R_{L1} - R_{L2})}{R_{L1} \times X_{L2} - X_{L1} \times R_{L2}}\right] + i \times \pi \quad i = 0, 1, 2 \ldots \quad (3)$$

Here, θ_1 is defined at the frequency of f_0 $(= f_1 + f_2)$. Obviously, "i" should be chosen properly so that $\theta_1 > 0$. Generally, "i" is determined taking two factors into consideration, the dimension of transmission line and the input impedance transformed (Z_{in1} in Figure 1). A proper value of "i" should be selected so that the transmission line is easy to fabricate and the impedance transformed makes an advantageous prerequisite for the next processes.

Once TL1 is determined, the basic impedance transforming formula can be employed to calculate the value of Z_{in1}

$$Z_{in1} = Z_1 \times \frac{Z_L + j \times Z_1 \times \tan\theta}{Z_1 + j \times Z_L \times \tan\theta} \quad (4)$$

In (4), θ stands for the corresponding electrical length at a frequency. Apply (4) at f_1 and f_2, the impedances transformed at both frequencies can be determined.

Here, since the electrical length of a transmission line is proportional to operating frequency, the value of Z_{in1} should be obtained using the following two equations

$$Z_{in1} = \begin{cases} Z_1 \times \dfrac{Z_{L1} + j \times Z_1 \times \tan[p_1 \times \theta_1]}{Z_1 + j \times Z_{L1} \times \tan[p_1 \times \theta_1]} & \text{at } f_1 \\[3mm] Z_1 \times \dfrac{Z_{L2} + j \times Z_1 \times \tan[p_2 \times \theta_1]}{Z_1 + j \times Z_{L2} \times \tan[p_2 \times \theta_1]} & \text{at } f_2 \end{cases} \quad (5)$$

In the equations above, p_1 and p_2 are defined as the fractions of each frequency to the sum frequency.

$$\begin{cases} p_1 = \dfrac{f_1}{f_1 + f_2} \\[3mm] p_2 = \dfrac{f_2}{f_1 + f_2} \end{cases} \quad (6)$$

As discussed above, the values of Z_{in1} at the two frequencies are conjugate. That is to say, after the transformation of TL1, the input

impedances follow the following form:

$$Z_{in1} = \begin{cases} R_{in1} + j \times X_{in1} \text{ at } f_1 \\ R_{in1} - j \times X_{in1} \text{ at } f_2 \end{cases} \tag{7}$$

2.2. Analysis of the Possible Locations of Z_{in1}

After the transformation of TL1, we get a pair of impedances. When the impedances are symbolized in Smith chart, they should be symmetrical with respect to the horizon axis standing for pure real impedance.

Now, what is cared about in this paper is which section of the Smith chart encloses the impedances. Considering the possible results
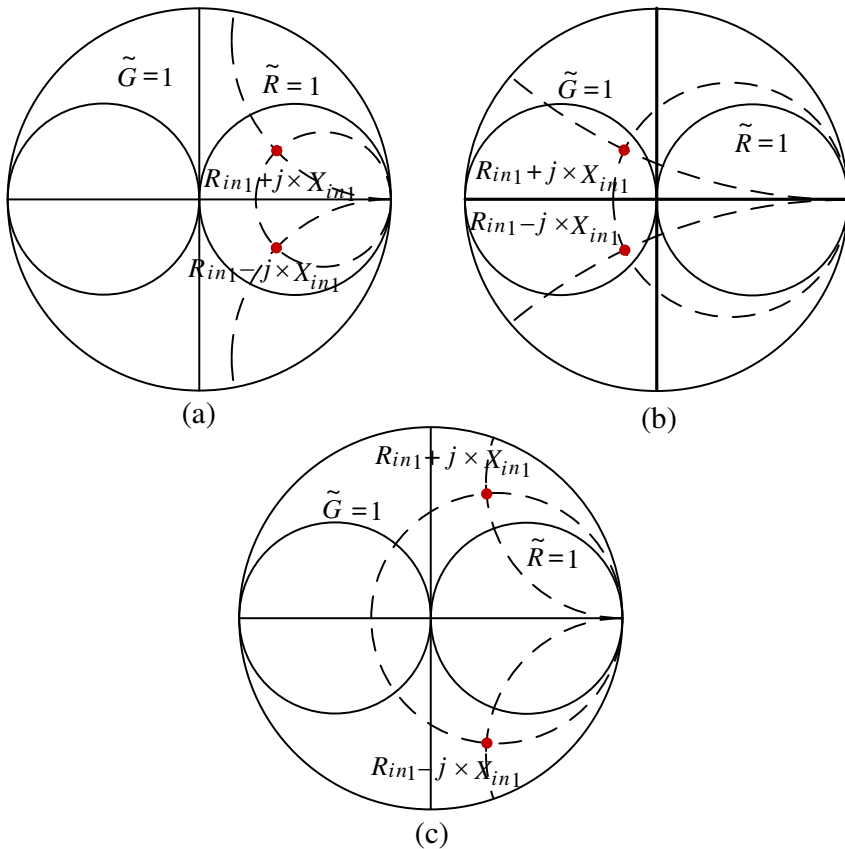

Figure 2. The three possible locations of Z_{in1}: (a) $\tilde{R} > 1$; (b) $\tilde{G} > 1$; (c) $\tilde{R} \le 1$ and $\tilde{G} \le 1$.

Smith chart can be divided into three sections. Figure 2 shows the separation of Smith chart according to possible locations of Z_{in1}.

Here, the Smith chart is divided into three sections. Using $\tilde{R}$ and $\tilde{G}$ as the normalized (normalized by Z_0) resistance and conductance, respectively, the three sections can be described as $\tilde{R} > 1$, $\tilde{G} > 1$, and the remnant (including the boundaries $\tilde{R} = 1$ and $\tilde{G} = 1$). Different analysis should be performed in each situation.

2.2.1. Case 1

In this case, Z_{in1} is located inside the circle of $\tilde{R} = 1$ (Figure 2(a)). Now let's take one of the impedances into consideration, for instance, the impedance at f_1 which is $R_{in1} + j \times X_{in1}$. We can always find a transmission line bearing specific characteristic impedance Z_{T1} as well as a special electrical length θ_{T1} to transform the impedance to $Z0$. This is shown in Figure 3.

Now let's consider the process of transforming $R_{in1} + j \times X_{in1}$ to Z_0 by employing only one transmission line, which is shown in Figure 4.

Assume the conjugate matching is achieved. Z'_{in1}, which is the input impedance when looking leftward in the right edge of the transmission line should be conjugate with $R_{in1} + j \times X_{in1}$. Thus the following equation should be satisfied:

$$Z'_{in1} = Z_{T1} \times \frac{Z_0 + j \times Z_{T1} \times \tan\theta_{T1}}{Z_{T1} + j \times Z_0 \times \tan\theta_{T1}} = R_{in1} - j \times X_{in1} \qquad (8)$$

Rearrange the equation above and separate the real part and imaginary part in both sides. The following two independent equations
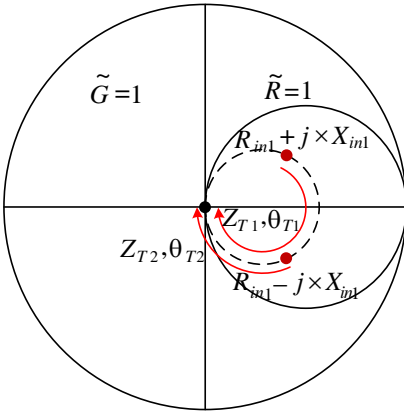

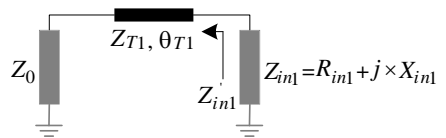**Figure 3.** A sketch for match Z_{in1} to Z_0 when $R_{in1} > 1$.

Figure 4. A single transmission line used to match Z_{in1} to Z_0.

can be obtained:

$$\begin{cases} Z_{T1} \times Z_0 = R_{in1} \times Z_{T1} + X_{in1} \times Z_0 \times \tan\theta_{T1} & \text{from real part} \\ Z_{T1}^2 \times \tan\theta_{T1} = R_{in1} \times Z_0 \times \tan\theta_{T1} - Z_{T1} \times X_{in1} & \text{from imaginary part} \end{cases} \quad (9)$$

It is easy to obtain the solutions of the equations above:

$$\begin{cases} Z_{T1} = \sqrt{\dfrac{X_{in1}^2 \times Z_0}{R_{in1} - Z_0} + R_{in1} \times Z_0} \\ \theta_{T1} = \arctan\left[\dfrac{Z_{T1} \times (R_{in1} - Z_0)}{X_{in1} \times Z_0}\right] + q \times \pi \end{cases} \quad (10)$$

Here, "q" is an integer and should be chosen properly so that θ_{T1} is involved in range $(0, \pi)$. The other impedance $R_{in1} - j \times X_{in1}$ can be analyzed in the same way. We can easily get Z_{T2} and θ_{T2} by replace "X_{in1}" with "$-X_{in1}$" because of the conjugate relation between the two impedances. Then we get the relations between Z_{T1} and Z_{T2} as well as θ_{T1} and θ_{T2}, respectively.

$$\begin{cases} Z_{T2} = Z_{T1} \\ \theta_{T1} + \theta_{T2} = \pi \end{cases} \quad (11)$$

2.2.2. Case 2

This time, Z_{in1} is located in the area $\tilde{G} > 1$ (Figure 2(b)). We can still use the methodology in case 1 to get the relations between Z_{T1} and
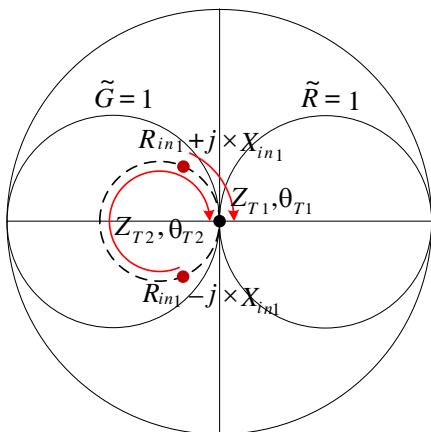

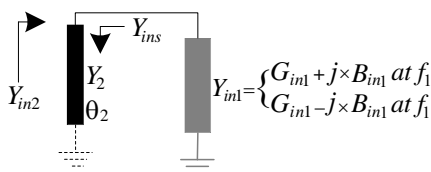**Figure 5.** A sketch for match Z_{in1} to Z_0 when $G_{in1} > 1$.

Figure 6. The analysis of TL2.

Z_{T2} as well as θ_{T1} and θ_{T2}. So (11) is still satisfied. In case 2 the value of Z_{T1} (= Z_{T2}) is smaller than Z_0, while in case 1, it's larger than Z_0. Figure 5 shows the sketch of the matching, where G_{in1} stands for the conductance of Z_{in1}.

2.2.3. Case 3

If Z_{in1} is not located in area of $\tilde{R} > 1$ nor $\tilde{G} > 1$. (Figure 2(c)) There won't be a single transmission line that is able to transform Z_{in1} to Z_0. Then, an extra stub should be taken into use. As shown in Figure 1, TL2 is added before the next process.

TL2 may be an open stub or a short stub. Here all impedances are turned to admittances. As Figure 6 shows, with characteristic admittance of Y_2 and electrical length of θ_2 (at frequency $f = f_1 + f_2$), the input admittances of the stub are obtained:

$$\text{open stub} : \begin{cases} Y_{ins1} = j \times Y_2 \times \tan[p_1 \times \theta_2] \text{ at frequency } f_1 \\ Y_{ins2} = j \times Y_2 \times \tan[p_2 \times \theta_2] \text{ at frequency } f_2 \end{cases} \quad (12)$$

$$\text{short stub} : \begin{cases} Y_{ins1} = -j \times Y_2 \times \cot[p_1 \times \theta_2] \text{ at frequency } f_1 \\ Y_{ins2} = -j \times Y_2 \times \cot[p_2 \times \theta_2] \text{ at frequency } f_2 \end{cases} \quad (13)$$

Here, the footnote "$ins1$" and "$ins2$" denote the two frequencies. By properly choosing an extra stub, Z_{in1} is transformed into Z_{in2}, and Z_{in2} should be inside the circle $\tilde{R} = 1$ and keep conjugate at the two frequencies, thus the analysis in case 1 is available. In (12) and (13), "p_1" and "p_2" are defined in (6), so $p_1 + p_2 = 1$ is satisfied. Now if we choose θ_2 to be π, the input admittance at one frequency will be opposite number of input admittance at the other frequency. Then Y_{in2} can be determined.

$$Y_{ins1} = -Y_{ins2} \quad (14)$$

$$Y_{in2} = \begin{cases} G_{in1} + j \times B_{in1} + Y_{ins1} \text{ at } f_1 \\ G_{in1} - j \times B_{in1} + Y_{ins2} \text{ at } f_2 \end{cases} \quad (15)$$

As a consequence, the two values of Y_{in2} at the two frequencies will be conjugate. Here, Y_2 is not fixed, but Z_{in2} will vary with the value of Y_2 and thus affects the coming process. Besides, the stub is chosen open or short based on the locations of Z_{in1} at the two frequencies. Figure 7 is an example in which an open stub is employed. Here, Z_{in1} at f_1 is inductive while Z_{in1} at f_2 is capacitive.

By resorting to TL2, Z_{in1} is transformed to Z_{in2} and thus able to be analyzed using the same methodology in case 1.
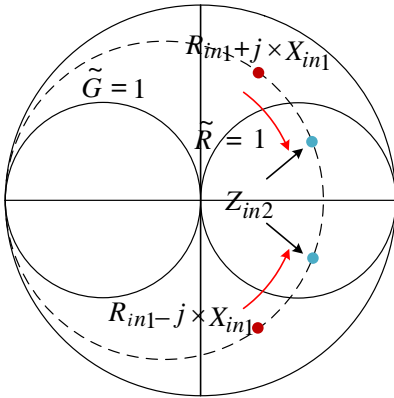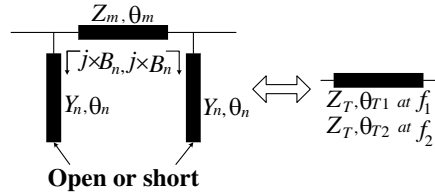
Figure 7. An example showing the function of TL2.

Figure 8. Topology of the Pi-section structure.

2.3. Pi-section Structure

Once Z_{in2} meets the requirement of case 1 or case 2 (in case 1 and 2, TL2 doesn't exist and Z_{in2} is equal to Z_{in1}), We can always find two transmission lines transforming Z_{in2} to Z_0 at the two frequencies, respectively. As illustrated above, the electrical length of the transmission lines at the two frequencies (θ_{T1} and θ_{T2}) should sum to π and the characteristic impedances at the two frequencies should be identical. The problem lies in that a single transmission line which meets the requirements doesn't exist, because θ_{T1} and θ_{T2} are independent from frequencies. So an equivalent structure is needed.

In this paper, a Pi-section structure is designed to act as a transmission line that bears the characteristics discussed above. The Pi-section structure is shown in Figure 8.

The Pi-section structure consists of three transmission lines, a serial transmission line and two identical stubs. The serial line has a characteristic impedance of Z_m and electrical length of θ_m. And each stub contributes an input admittance of $j \times B_n$. Since Pi-section structure is composed of three serial sections, $ABCD$ matrix provides a good way to analyze the structure. By equalizing the $ABCD$ matrix of the Pi-section structure and that of the single transmission line, some equations may be constructed and solved.

The $ABCD$ matrix of the Pi-section is presented when multiplying the three individual $ABCD$ matrices

$$A_\pi = A_1 \times A_2 \times A_3 = \begin{bmatrix} 1 & 0 \\ j \times B_n & 1 \end{bmatrix} \times \begin{bmatrix} \cos\theta_m & j \times Z_m \times \sin\theta_m \\ j \times \frac{\sin\theta_m}{Z_m} & \cos\theta_m \end{bmatrix} \times \begin{bmatrix} 1 & 0 \\ j \times B_n & 1 \end{bmatrix}$$

$$= \begin{bmatrix} \cos\theta_m - B_n \times Z_m \times \sin\theta_m \\ j \times \frac{\sin\theta_m}{Z_m} \times \left(1 - Z_m^2 \times B_n^2 + 2 \times Z_m \times B_n \times \cot\theta_m\right) \end{bmatrix}$$

$$\begin{array}{c} j \times Z_m \times \sin\theta_m \\ \cos\theta_m - B_n \times Z_m \times \sin\theta_m \end{array} \Bigg] \tag{16}$$

Here, "A_2" represents the $ABCD$ matrix of serial transmission line of the Pi-section structure. "A_1" and "A_3" are the $ABCD$ matrices of the two stubs.

Meanwhile, a single transmission line has $ABCD$ matrix as follow:

$$A_T = \begin{bmatrix} \cos\theta_T & j \times Z_T \times \sin\theta_T \\ j \times \frac{\sin\theta_T}{Z_T} & \cos\theta_T \end{bmatrix} \tag{17}$$

Here, Z_T and θ_T stand for the characteristic impedance and the electrical length of a transmission line, respectively. Equalize every element in A_π and A_T, respectively. Three equations are obtained:

$$\cos\theta_m - B_n \times Z_m \times \sin\theta_m = \cos\theta_T \tag{18}$$

$$j \times Z_m \times \sin\theta_m = j \times Z_T \times \sin\theta_T \tag{19}$$

$$j \times \frac{\sin\theta_m}{Z_m} \times \left(1 - Z_m^2 \times B_n^2 + 2 \times Z_m \times B_n \times \cot\theta_m\right) = j \times \frac{\sin\theta_T}{Z_T} \tag{20}$$

It seems that we have to solve three equations, however, (20) is not an independent equation. Once (18) and (19) are obtained, (20) will always be exact. Here is the demonstration.

From (18), we get the following equation:

$$B_n \times Z_m = \frac{\cos\theta_m - \cos\theta_T}{\sin\theta_m} \tag{21}$$

Substitute (21) into (20) and the left side of the equal sign is transformed to:

$$j \times \frac{\sin\theta_m}{Z_m} \times \left[1 - \left(\frac{\cos\theta_m - \cos\theta_T}{\sin\theta_m}\right)^2 + 2 \times \frac{\cos\theta_m - \cos\theta_T}{\sin\theta_m} \times \cot\theta_m\right] \tag{22}$$

After been simplified, (22) becomes the following formula:

$$j \times \frac{\sin^2\theta_T}{Z_m \times \sin\theta_m} \tag{23}$$

Then, use (19), the equation above is transformed to be $j \times \sin\theta_T/Z_T$, which happens to be the right side of the equal sign in (20). As a consequence, we have only two independent Equations (18) and (19).

Now equations should be applied at the two operating frequencies.

From Equation (19), the electrical lengths at the two frequencies satisfy the following formula:

$$\sin\theta_{m1} = \frac{Z_T \times \sin\theta_{T1}}{Z_m} \tag{24}$$

$$\sin\theta_{m2} = \frac{Z_T \times \sin\theta_{T2}}{Z_m} \tag{25}$$

The footnotes "$m1$" and "$m2$" denotes the frequencies f_1 and f_2, respectively. And we have known that $\theta_{T1} + \theta_{T2} = \pi$. Then, $\sin\theta_{m1}$ is always equal to $\sin\theta_{m2}$, that means

$$
\begin{aligned}
&\theta_{m1} + \theta_{m2} = k \times \pi \quad k = 1, 3, 5\ldots \quad \text{(case a)}\\
&\text{or} \\
&\theta_{m2} - \theta_{m1} = l \times \pi \quad l = 2, 4, 6\ldots \quad \text{(case b)}
\end{aligned}
\tag{26}
$$

To obtain a smaller dimension, case a should be chosen. What's more, k should be the smallest available value, $k = 1$. That means, the electrical length at frequency $f_0(= f_1 + f_2)$ is π. Hence, $\theta_{m1} = p_1 \times \pi$, and $\theta_{m2} = p_2 \times \pi$.

Then Z_m can be determined following equation derived from (19):

$$Z_m = \frac{Z_T \times \sin\theta_{T1}}{\sin\theta_{m1}} \tag{27}$$

Now rewrite Equation (18) at each frequency.

$$\cos\theta_{m1} - B_{n1} \times Z_m \times \sin\theta_{m1} = \cos\theta_{T1} \tag{28}$$
$$\cos\theta_{m2} - B_{n2} \times Z_m \times \sin\theta_{m2} = \cos\theta_{T2} \tag{29}$$

The footnotes "$n1$" and "$n2$" denote the two frequencies f_1 and f_2. Here, $\cos\theta_{T1}$ is the opposite number of $\cos\theta_{T2}$, so the following equation should always be satisfied:

$$\cos\theta_{m1} - B_{n1} \times Z_m \times \sin\theta_{m1} = -(\cos\theta_{m2} - B_{n2} \times Z_m \times \sin\theta_{m2}) \tag{30}$$

Consider the following relations:

$$\cos\theta_{m1} = -\cos\theta_{m2} \tag{31}$$
$$\sin\theta_{m1} = \sin\theta_{m2} \tag{32}$$

If only B_{n1} is the opposite number of B_{n2}, (30) can always be satisfied. As the input admittances of the stubs can be described as:

$$\text{open stub}: \begin{cases} B_{n1} = Y_n \times \tan\theta_{n1} \text{ at frequency } f_1 \\ B_{n2} = Y_n \times \tan\theta_{n2} \text{ at frequency } f_2 \end{cases} \tag{33}$$

$$\text{short stub}: \begin{cases} B_{n1} = -Y_n \times \cot\theta_{n1} \text{ at frequency } f_1 \\ B_{n2} = -Y_n \times \cot\theta_{n2} \text{ at frequency } f_2 \end{cases} \tag{34}$$

In order to make B_{n1} opposite to B_{n2}, the following relation should be satisfied:

$$\tan\theta_{n1} = -\tan\theta_{n2} \quad \text{or} \quad \cot\theta_{n1} = -\cot\theta_{n2} \tag{35}$$

From which we can get the following:

$$\theta_{n1} + \theta_{n2} = r \times \pi \quad r = 1, 2, 3\ldots \tag{36}$$

Usually, "r" is chosen to be 1 for miniaturization's sake. That means the electrical length of the stub is π at frequency $f_0(= f_1 + f_2)$. Hence, $\theta_{n1} = p_1 \times \pi$, and $\theta_{n2} = p_2 \times \pi$.

With the electrical length of the stubs determined, B_{n1} can be calculated by applying (18) at frequency f_1.

$$B_{n1} = \frac{\cos\theta_{m1} - \cos\theta_{T1}}{Z_m \times \sin\theta_{m1}} \tag{37}$$

If $B_{n1} > 0$, the subs should be open, the characteristic admittance is determined by:

$$Y_n = \frac{\cos\theta_{m1} - \cos\theta_{T1}}{\tan\theta_{n1} \times Z_m \times \sin\theta_{m1}} \tag{38}$$

If $B_{n1} < 0$, the stubs are short, then Y_n is calculated from:

$$Y_n = -\frac{\cos\theta_{m1} - \cos\theta_{T1}}{\cot\theta_{n1} \times Z_m \times \sin\theta_{m1}} \tag{39}$$

In special case, $B_{n1}=0$, that means the following equation is satisfied:

$$\frac{\theta_{T1}}{\theta_{T2}} = \frac{f_1}{f_2} \tag{40}$$

In this case, the stubs of Pi-section are no longer needed, and a single transmission line is able to transform Z_{in2} to Z_0 at both the frequencies.

3. NUMERICAL EXAMPLES

To verify the proposed impedance transformer, several examples for dual-band matching are presented. All of the impedances are derived from simulation based on GaN HEMT CGH40010. The impedances may be used in input matching or output matching.

The parameters of the proposed impedance transformer in different situations are tabulated in Table 1.

Here, case 1 and case 3 are for input matching networks. Case 2 and case 4 are for output matching networks. θ_1 is determined at frequency $f_0(= f_1 + f_2)$. θ_2, θ_m, and θ_n which are not mentioned in the table are all 180° at frequency f_0. $Z_2 = 1/Y_2$, and "/" means TL2 is not necessary, which indicates that case 1 and case 2 in Section 2.2 is obtained when evaluating the value of Z_{in1}. Z_0 is 50 Ω in all cases.

Table 1. Numerical examples of the transformer.

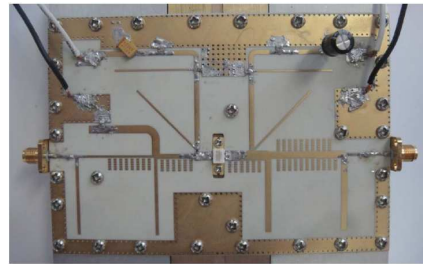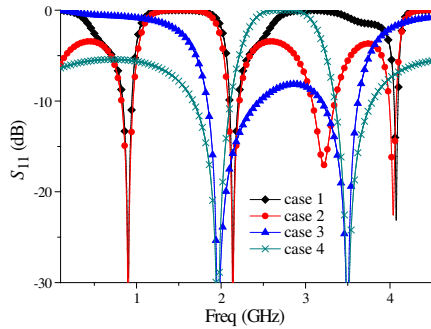|	case 1	case 2	case 3	case 4
$f_1/$GHz	0.9	0.9	1.96	1.96
$f_2/$GHz	2.14	2.14	3.5	3.5
R_{L1}/Ω	47.088	9.734	4.699	18.993
X_{L1}/Ω	−55.200	4.230	−3.248	−8.247
R_{L2}/Ω	11.063	8.385	7.131	16.315
X_{L2}/Ω	−10.289	−0.575	−33.9008	1.503
Z_1/Ω	36.3082	22.2133	47.1479	26.612
$\theta_1/$angle	84.4895	102.188	40.1085	23.6035
Z_2/Ω (O/S)	26 (S)	/	/	/
Z_m/Ω	57.429	29.1497	11.2026	30.3126
Z_n/Ω (O/S)	49.0735 (O)	31.626 (O)	27.9839 (S)	79.1106 (O)

Figure 9. Simulated return loss of the examples.

Figure 10. Photograph of the 0.9/2.14 GHz power amplifier.

The symbol "O" and "S" in the bracket following some characteristic impedances denote open stubs and short stubs, respectively. Simulation is performed based on the parameters in Table 1. Figure 9 shows the simulated return loss of the numerical examples.

4. EXPERIMENT

In this paper, a 0.9/2.14 GHz dual-band power amplifier is designed based on the dual-band impedance transformer proposed. The
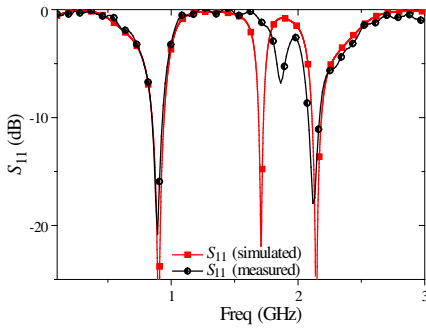
Figure 11. Simulated and measured return loss of the 0.9/2.14 GHz power.
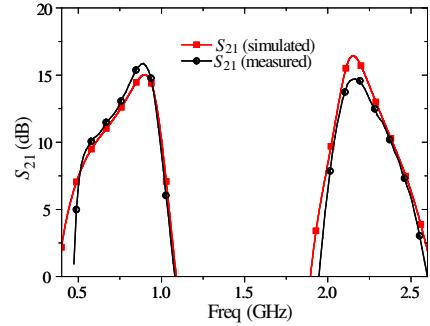
Figure 12. Simulated and measured small signal gain of the 0.9/2.14 GHz power amplifier.

input/output matching networks are fabricated using the parameters in Table 1. In addition, extra circuits for DC bias, stability and DC block are employed. Here, the short end of TL2 is realized through two parallel capacities bearing two resonance frequencies those happen to be the operating frequencies. The photograph of the amplifier is shown in Figure 10. The PA is fabricated using RO4350B (ε_r = 3.48, thickness = 20 mil, 1 oz. copper). The proposed PA was measured using Agilent Network Analyzer. Figures 11 and 12 show the reflection coefficient (S_{11}) and the small signal gain (S_{21}), respectively. In each figure, a comparison between simulation and measurement is performed. From the comparison, a good accordance between simulation and measurement is obtained.

5. CONCLUSION

In this paper, a new methodology for dual-band frequency-dependent complex impedance matching is proposed. Closed-form equations are obtained after analyzing the structure in detail. In addition, a 900/2140 MHz power amplifier was realized using the proposed methodology. A good agreement between simulation and measurement is obtained, which substantiates the validity of the dual-band impedance transformer.

REFERENCES

1. Li, B., X. Wu, N. Yang, and W. Wu, "Dual-band equal/unequal Wilkinson power dividers based on coupled-line section with short-circuited stub," *Progress In Electromagnetics Research*, Vol. 111, 163–178, 2011.

2. Kuo, J.-T., C.-Y. Fan, and S.-C. Tang, "Dual-wideband bandpass filters with extended stopband based on coupled-line and coupled three-line resonators," *Progress In Electromagnetics Research*, Vol. 124, 1–15, 2012.

3. Jiménez-Martín, J. L., V. González-Posadas, J. E. González-García, F. J. Arques-Orobon, L. E. Garcia-Munoz, and D. Segovia-Vargas, "Dual band high efficiency class CE power amplifier based on CRLH diplexer," *Progress In Electromagnetics Research*, Vol. 97, 217–240, 2009.

4. Wei, K. P., Z. Zhang, and Z. Feng, "Design of a dual-band omnidirectional planar microstrip antenna array," *Progress In Electromagnetics Research*, Vol. 126, 101–120, 2012.

5. Cheng, K.-K. M. and F.-L. Wong, "A novel approach to the design and implementation of dual-band compact planar 90° branch line coupler," *IEEE Transactions on Microwave Theory and Techniques*, Vol. 52, No. 11, 2458–2463, 2004.

6. Chen, X.-Q., X.-W. Shi, Y.-C. Guo, and M.-X. Xiao, "A novel dual band transmitter using microstrip defected ground structure," *Progress In Electromagnetics Research*, Vol. 83, 1–11, 2008.

7. Rawat, K., M. S. Hashmi, and F. M. Ghannouchi, "Dual-band RF circuits and components for multi-standard software defined radios," *IEEE Circuits and Systems Magazine*, Vol. 12, No. 1, 12–32, 2012.

8. Chow, Y. L. and K. L. Wan, "A transformer of one-third wavelength in two sections — For a frequency and its first harmonic," *IEEE Microwave and Wireless Components Letters*, Vol 12, No. 1, 22–23, 2002.

9. Monon, C., "A small dual frequency transformer in two sections," *IEEE Transactions on Microwave Theory and Techniques*, Vol. 51, No. 4, 1157–1161, 2003.

10. Orfanidis, S. J., "A two-section dual-band Chebyshev impedance transformer," *IEEE Microwave and Wireless Components Letters*, Vol. 13, No. 9, 382–384, 2003.

11. Castaldi, G., V. Fiumara, and I. Gallina, "An exact synthesis method for dual-band Chebyshev impedance transformers," *Progress In Electromagnetics Research*, Vol. 86, 305–319, 2008.

12. Wu, Y., Y. Liu, and S. Li, "A compact Pi-structure dual band transformer," *Progress In Electromagnetics Research*, Vol. 88, 121–134, 2008

13. Colantonio, P., F. Giannini, and L. Scucchia, "A new approach to design matching networks with distributed elements," *15th International Conference on Microwaves, Radar and Wireless Communications, MIKON-2004*, Vol. 3, 811–814, 2004.

14. Ji, S. H., C. S. Cho, J. W. Lee, and J. Kim, "Concurrent dual-band class-E power amplifier using composite right/left-handed transmission lines," *IEEE Transactions on Microwave Theory and Techniques*, Vol. 55, No. 6, 1341–1347, 2007.

15. Liu, X., Y. A. Liu, S. L. Li, F. Wu, and Y. L. Wu, "A three-section dual band transformer for frequency-dependent complex load impedance," *IEEE Microwave and Wireless Components Letters*, Vol. 19, No. 10, 611-613, 2009.

16. Nikravan, M. A. and Z. Atlasbaf, "T-section dual-band impedance transformer for frequency-dependent complex loads," *Electronics Letters*, Vol. 47, No. 9, 551–553, 2011.

17. Rawat, K. and F. M. Ghannouchi, "Dual-band matching technique based on dual-characeristic impedance transformers for dual-band power amplifier design," *IET Microwaves, Antennas & Propagation*, Vol. 5, No. 14, 1720–1729, 2011.

18. Chuang, M.-L., "Dual-band impedance transformer using two-section shunt stubs," *IEEE Transactions on Microwave Theory and Techniques*, Vol. 58, No. 5, 1257–1263, 2010.

19. Wu, Y. L., Y. A. Liu, and S. L. Li, "A dual-frequency transformer for complex impedances with two unequal sections," *IEEE Microwave and Wireless Components Letters*, Vol. 19, No. 2, 77–79, 2009.

20. Liu, Y., Y.-J. Zhao, and Y. Zhou, "Lumped dual-frequency impedance transformers for frequency-dependent complex loads," *Progress In Electromagnetics Research*, Vol. 126, 121–138, 2012.

21. Fagotti, R., A. Cidronali, and G. Manes, "Concurrent hex-band GaN power amplifier for wireless communication systems," *IEEE Microwave and Wireless Components Letters*, Vol. 21, No. 2, 89–91, 2011.